Ejection of a Large Neutral Cluster from a Liquid Beam Surface Following IR Laser Irradiation

Jun-ya Kohno, Fumitaka Mafuné,† and Tamotsu Kondow*

East Tokyo laboratory, Genesis Research Institute, Inc., and Cluster Research Laboratory, Toyota Technological Institute, 717-86 Futamata, Ichikawa, Chiba 272-0001, Japan

Received: August 7, 2003; In Final Form: October 23, 2003

A continuous liquid flow of water in a vacuum (a liquid beam) was irradiated with a pulsed IR laser at 2.96 μm that is resonant to an OH stretching mode of liquid water. Neutral species ejected from the liquid beam were detected directly by a Daly detector without ionization. The flight-time distribution was found to show neutral species having high and low velocities, which are attributable to water clusters ejected from the surface and inside of the liquid beam, respectively. The flight-time distribution expressed by a Maxwellian velocity distribution reveals that the clusters are ejected by explosion of the liquid beam after absorption of the IR laser. This ejection scheme is supported by the presence of a delayed ejection of clusters, which is considered to originate from the inside of the liquid beam into the gas phase.

1. Introduction

Liquid is an ideal system for a mechanistic study of laser ablation, because liquid is microscopically homogeneous and isotropic. Srinivasan and Ghosh have shown that ablation of liquid benzene by a 248-nm laser pulse is regarded to be photochemical decomposition following two-photon absorption.[1] Masuhara and co-workers have elucidated that photochemical and photothermal mechanisms are operative in UV-laser ablation of solutions containing aromatic molecules. In the photochemical mechanism, chemical reactions of photodegradated products induce ejection of materials, whereas in the photothermal mechanism, nonradiative relaxation of the chromophore gives rise to the ejection because of a temperature rise of the solution by the relaxation.[2−5]

The mechanism of the laser ablation is most adequately investigated by a mass spectrometric method, because detailed information is provided by analyzing the velocity distributions of product species in a vacuum. The investigations of this kind are very limited because of the difficulty of making a smooth surface of a volatile liquid inside a vacuum chamber. Therefore, it is customary to deal with nonvolatile liquids to get rid of the difficulty as investigated by Furlan and co-workers.[6,7] Recent progress on the technique of a liquid beam (a continuous liquid flow in a vacuum) allows us to investigate various volatile liquids in the vacuum chamber.[8,9] Brutschy and co-workers have observed various solute ions by irradiating an IR laser onto a liquid beam.[10−15] Abel and co-workers have recently produced protonated amino acids by shining an IR laser onto the liquid beam as well.[16] On the other hand, we have investigated the mechanism of IR-laser ablation on a liquid beam of an aqueous solution of phenol and have revealed that fast and internally cold phenol−water clusters are ejected from a surface region of the beam at an early time after the laser ablation, while slow but internally hot phenol−water clusters are evaporated from the whole region of the beam at a later time; they are named as impulsive and thermal ejection, respectively.[17−19] The impulsive ejection tends to be favored to an increasing extent with increase in the laser fluence. We have also reported that more intense IR-laser irradiation produces large clusters in the gas phase.[20] In the present paper, we report velocity measurements of water clusters produced from a liquid beam of water under irradiation of an intense IR-laser whose power is in the range of 4−8 mJ/pulse, and show that large water clusters are produced from the surface and the inside of the liquid beam with different velocity distributions.

2. Experimental Section

Figure 1 shows a schematic diagram of the apparatus employed in the present study. A continuous laminar liquid flow of a sample solution was introduced into a vacuum chamber from a nozzle having an aperture with a diameter of 20 μm. A constant liquid flow was supplied by a Shimadzu LC-6A pump designed for a liquid chromatograph. The flow rate was maintained at 0.2 mL/min with a pressure of typically 20 atm inside the nozzle. The source chamber was evacuated down to 10^{-5}−10^{-6} Torr by a 1200 L s^{-1} diffusion pump and a liquid N_2 trap during injection of the liquid beam. Commercially available water (deionized and distilled) and aniline were used without further purification.

The liquid beam was crossed with a pulsed IR laser (2.96 μm) at a distance of 2 mm downstream from the nozzle. The wavelength of the IR laser is resonant to the OH stretching vibration of liquid water. The IR laser beam was generated by an INRAD IR-OPO system and was focused by a lens with a focal length of 775 mm. The power of the IR laser (4−8 mJ/pulse) was monitored by an OPHIR ELECTRONICS laser energy meter.

Neutral clusters ejected from the liquid beam under the IR laser irradiation were collimated by a 3-mm aperture placed 25 mm from the liquid beam, and were detected by a Daly multiplier mounted 1.65 m away from the liquid beam. In more detail, the clusters were admitted to an aluminum target floated up to ca. −20 kV against the ground, ionic species produced by the collision were allowed to collide onto an electrically grounded aluminized scintillator, and photons generated from it were detected by a photomultiplier. The signal from the Daly multiplier should originate from neutral species impinging on

* To whom correspondence should be addressed.
† Present address: Department of Basic Sciences, Graduate School of Arts and Sciences, The University of Tokyo, Komaba, Meguro-ku, Tokyo 152-8902, Japan.

10.1021/jp0363343 CCC: $27.50
Published on Web 01/15/2004

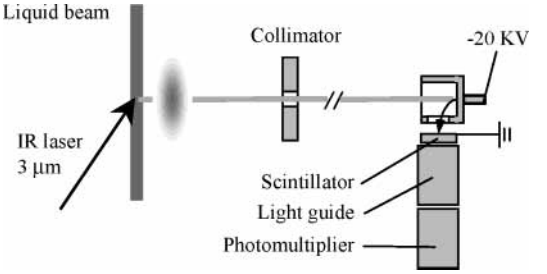

Figure 1. A schematic diagram of the apparatus.

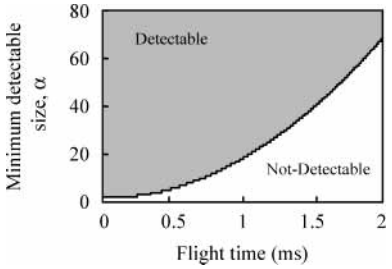

Figure 2. Minimum detectable size of neutral species as a function of the flight time.

the aluminum target, because the signal is insensitive to a retarding voltage of ±2 kV applied in the flight tube. Note that the detector starts to detect neutral particles when their kinetic energies exceed the work function of the aluminum target (4.28 eV[21]). The signals were collected in a pulse-counting mode.

The masses of the neutral species were estimated by adding aniline to the water as a chromophore, which is ionized by the UV laser (270 nm) obtained by frequency-doubling the output of a Quanta-ray PDL-3 dye laser pumped by the third harmonic of a Quanta-ray GCR-3 Nd:YAG laser. The UV laser was triggered at a delay time of 1 μs after the IR laser irradiation 0.5 mm from the liquid beam of a 0.2 M aqueous solution of aniline so as to ionize neutral species isolated by the IR laser. Ions produced by the UV-laser irradiation were accelerated by a pulsed electric field in the direction perpendicular to both the liquid and the laser beams after a given delay time (1 μs) from the UV-laser irradiation. The ions produced by the UV-laser ionization were detected by the Daly multiplier after being steered and focused by a set of vertical and horizontal deflectors and an einzel lens.

3. Analysis of Flight-Time Distributions

The flight-time distribution of neutral clusters provides their velocity distribution, because the distance between the liquid beam and the detector dynode is fixed throughout the measurements (1.65 m). The scheme of the IR-laser ablation is given by

$$H_2O\ (s) + h\nu_{IR} \rightarrow (H_2O)_n\ (g) \tag{1}$$

$$(H_2O)_n\ (g) \rightarrow (H_2O)_{n-1}\ (g) \rightarrow (H_2O)_{n-2}\ (g) \rightarrow ... \rightarrow (H_2O)_{n'}\ (g) \tag{2}$$

where (s) and (g) represent solution and gas phases, respectively. Water molecules in the liquid beam of a solution are liberated into the gas phase as water clusters, which undergo unimolecular dissociation before arriving at the detector. A water cluster, $(H_2O)_n$, just after its birth (nascent) is considered to be equilibrated with the surface of the liquid beam (process 1). Therefore, the flight-time distribution of $(H_2O)_n$ is given by the Maxwellian distribution as

$$f_n(t) = Nt^{-4} \exp\left(-\frac{nm_w}{2kT}\left(\frac{X}{t} - V\right)^2\right) \tag{3}$$

where t is the flight time of the water cluster, X is the distance from the liquid beam to the detector, T is the translational temperature of the cluster, m_w is the mass of H_2O, and N is a normalization factor so that $\int_0^\infty f_n(t)\ dt = 1$. The flight-time distribution of a water cluster, $(H_2O)_{n'}$, produced by unimolecular dissociation is identical with that of the nascent water cluster, and hence is given by eq 3, because the cluster travels with the same velocity even after it undergoes the unimolecular dissociation.[22]

The flight-time distribution is given by superposition of the flight times of $(H_2O)_n$ with different sizes. The flight-time distributions obtained experimentally are deconvoluted based on four assumptions (assumptions 1−4) as described below.

Let us assume that only the clusters having kinetic energy more than 4.28 eV (the work function of an aluminum metal, E(Al)) are detected with a detection efficiency independent of the kinetic energy of the clusters[23] (assumption 1). The minimum detectable size, α, is given as

$$\frac{1}{2}\alpha m_w\left(\frac{X}{t}\right)^2 = E(\mathrm{Al}) \tag{4}$$

where t represents the flight time of a given cluster. Figure 2 shows the minimum detectable size, α, as a function of the flight time. The minimum detectable size increases with an increase in the flight time. It is considered that the nascent clusters, $(H_2O)_n$, of $n \geq \alpha$ are detected because all the fragment species produced in the course of the evaporation have the same velocity so that they hit the detector at the same time. Therefore, the flight-time distribution observed, F, is given by the summation of the flight-time distribution of each cluster, $(H_2O)_n$ ($n \geq \alpha$) as

$$F(t) = \sum_{n\geq\alpha} A(n) f_n(t) = \sum_{n\geq\alpha} A(n) N(n) t^{-4} \exp\left(-\frac{nm_w}{2kT}\left(\frac{X}{t} - V\right)^2\right) \tag{5}$$

where $A(n)$ is the abundance of $(H_2O)_n$ at $t = 0$. We consider that the floating velocity, V, and the translational temperature, T, of the product clusters are independent of the cluster size, n, on the assumption that the product clusters are equilibrated by colliding with each other in the laser ablation plume (assumption 2). It is also assumed that the abundance of a nascent cluster decreases exponentially with an increase in its mass[24] as

$$A(m) = A_0 e^{-\lambda m} \tag{6}$$

where A_0 and λ are parameters (assumption 3). Note that λ is the reciprocal of the average mass of the nascent cluster because $\int_0^\infty mA(m)dm / \int_0^\infty A(m)\ dm = 1/\lambda$. Inserting eq 6 into eq 5, one obtains

$$F(t) = \sum_{n=\alpha}^{\infty} A_0 \exp(-\lambda n m_w) N(m) t^{-4} \exp\left(-\frac{nm_w}{2kT}\left(\frac{X}{t} - V\right)^2\right) \tag{7}$$

The normalization constant, $N(m)$, is given by

$$N = X^3\left(\frac{kTV}{m}\exp\left(-\frac{mV^2}{2kT}\right) + \left(\frac{\pi kT}{2m}\right)^{1/2}\left(\frac{kT}{m}+V^2\right)\left[1+\mathrm{erf}\left(\left(\frac{mV^2}{2kT}\right)^{1/2}\right)\right]\right)^{-1} \quad (8)$$

where erf(z) is the error function. The normalization constant, N, monotonically increases with an increase in m. To simplify the flight-time distribution (eq 7), N is approximated by a linear relation

$$N \cong p + qm \quad (9)$$

where $p = N(1000)$ and $q = [N(10000) - N(1000)]/[10000 - 1000]$ (assumption 4). Note that most of the product clusters distribute at the mass range between 1000 and 10000. This assumption does not ignore the fact that of the clusters with masses of less than 1000, more than 10000 are present. Actually, this approximation introduces a systematic error; the actual value of $N(500)$, $N(5000)$, and $N(15000)$ differs by 25%, 12%, and 12%, respectively, from those estimated from eq 9. Using this approximation, one simplifies eq 8 as

$$F(t) = \sum_{n=\alpha}^{\infty} A_0 \exp(-\lambda n m_w)(p + qnm_w)t^{-4} \times \exp\left(-\frac{nm_w}{2kT}\left(\frac{X}{t}-V\right)^2\right) = A_0 t^{-4}\left(p\frac{e^{-\alpha a}}{1-e^{-a}} + qm_w\frac{\alpha e^{-\alpha a} - (\alpha-1)e^{-(\alpha+1)a}}{(1-e^{-a})^2}\right) \quad (10)$$

where $a = (m_w/2kT)[(X/t) - V]^2 + \lambda$. Equation 10 gives the flight-time distribution of the neutral clusters which are equilibrated with the liquid surface.

4. Results

Figure 3 shows flight-time distributions of neutral clusters produced from a liquid beam of water by irradiation of an IR laser at different pulse energies of 4.5−7 mJ/pulse. Each flight-time distribution consists of fast and slow components (see Figure 3). The solid curves represent the fast and the slow components obtained by deconvolution of the measured flight-time distribution on the assumption that they are expressed by eq 10. The tail potion of the slow component is smaller than that measured. It is most probable that there are other components which contribute to the tail portion.

Figure 4 shows mass spectra of the ions produced from a 0.2 M aqueous solution of aniline under irradiation of IR and UV lasers. The IR laser with a power of 0.5−8 mJ/pulse was focused onto the liquid beam, while the UV laser with a power of ∼0.9 mJ/pulse was focused at a distance of 0.5 mm away from the liquid beam (see panels a through h). The peaks shown in panels a−c are assigned to hydrated aniline cluster ions, $AN^+(H_2O)_n$. It is likely that $AN^+(H_2O)_n$ are produced at the IR laser powers higher than 4 mJ/pulse (see panels d−h) as well, although the resolution of the mass spectrometer is not high enough to resolve the peaks of every product ion. Note that the mass spectra shown in Figure 4 do not represent the abundance of all the product clusters, because the UV laser ionizes only a small portion of the clusters, but more or less reflects the size distribution of the product clusters. Then, one can conclude that the average size of $AN^+(H_2O)_n$ increases as the IR laser power increases up to 4 mJ/pulse, and levels off above 4 mJ/pulse.

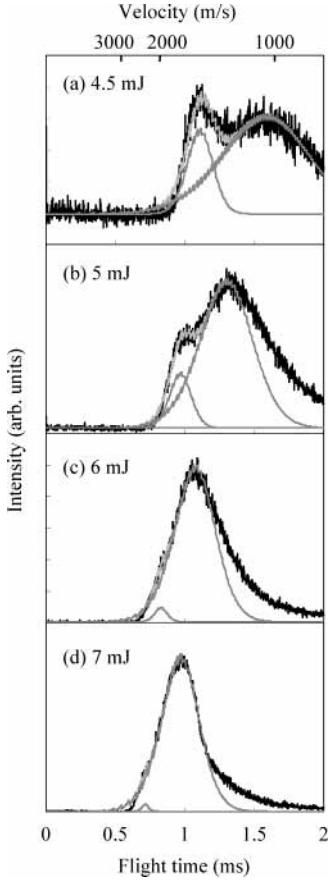

Figure 3. Flight-time distributions of product neutral species obtained by irradiation of an IR laser to a liquid beam of water. Powers of the incident IR laser are 4.5, 5, 6, and 7 mJ/pulse for panels a, b, c, and d, respectively. Solid curves show the fitted results to eq 10 (see text).

Figure 5g shows the flight-time distribution of neutral clusters produced from a 0.2 M aqueous solution of aniline under irradiation of an IR laser alone. On the other hand, panels a−f in Figure 5 show flight-time distributions of $AN^+(H_2O)_n$ under irradiation of both the IR and the UV lasers at different delay times (0.3−1.5 μs) between the timings of the IR and the UV laser irradiation, where no electric field was applied in the acceleration region. The IR laser was focused onto the liquid beam, whereas the UV laser was focused 0.5 mm away from it. The flight-time distribution obtained by irradiation of the IR laser alone (see panel g) was subtracted from those obtained by irradiation of both the IR and UV lasers, as shown in Figure 5, panels a−f. Namely, flight-time distributions a−f are given by the photoions produced by irradiation of the UV laser. The cluster ions travel in the gas phase with the same velocity before the ionization, because no electric field is applied in the ionization region. The flight-time distributions exhibit an intense peak in addition to a small side peak (panels b and c). The flight time increases with increase in the IR−UV delay time.

Fitting each component with eq 10 (solid curves in Figure 3), one obtains the abundance, A, the floating velocity, V, the translational temperature, T, and the reciprocal of the average mass, λ, of each component.[25] These are independent parameters, so that one can determine the parameters uniquely from one flight-time distribution. The abundances of the two components are calculated by integrating eq 10 with the flight time, t. Figure 6 shows the abundances of the two components as a function of the incident IR laser power. As the laser power increases, the abundances of both the slow and the fast components start to rise at a threshold laser power (∼ 4 mJ/

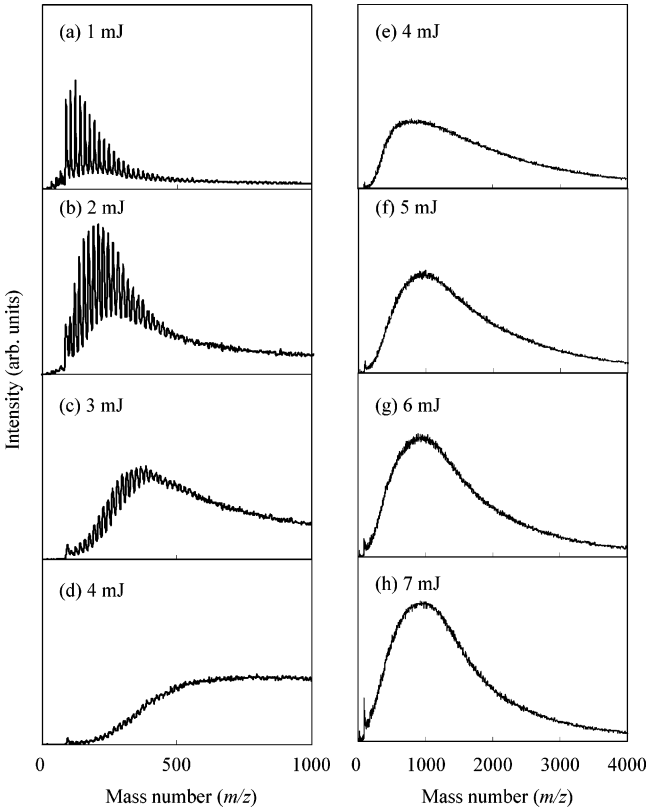

Figure 4. Mass spectra of the ions produced from a 0.2 M aqueous solution of aniline under irradiation of IR and UV lasers. The IR laser is focused onto the liquid beam, whereas the UV laser is focused 0.5 mm away from the liquid beam. The power of the IR laser is 1, 2, 3, and 4 mJ/pulse for panels a, b, c, and d, respectively, and 4, 5, 6, and 7 mJ/pulse for panels e, f, g, and h, respectively.

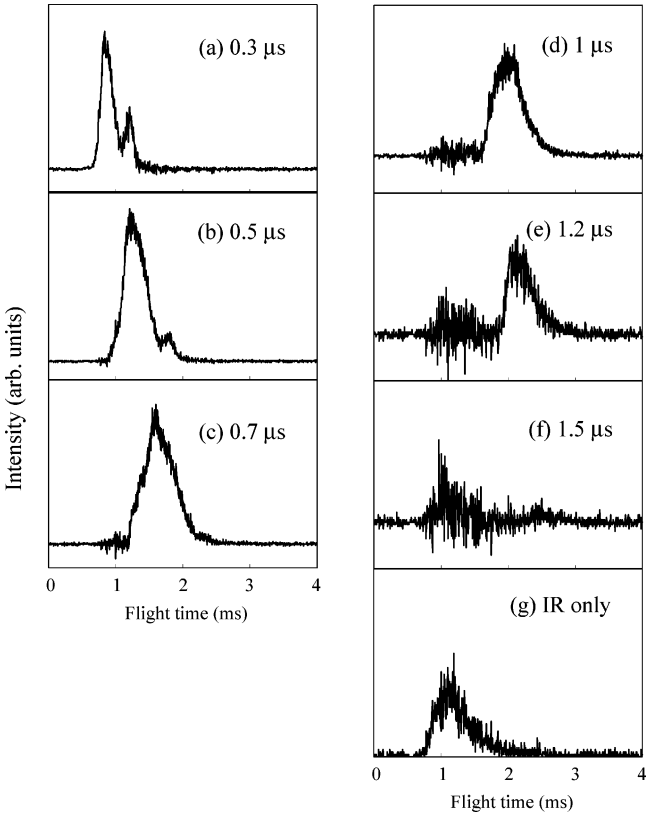

Figure 5. Flight-time distributions measured under irradiation of an IR laser (panel a) and under irradiation of an IR laser and a UV laser (panels b−g). The sample solution employed is a 0.2 M aqueous solution of aniline. The IR and the UV lasers are focused onto the liquid beam and 0.5 mm away from the liquid beam, respectively. The delay times from the IR laser to the UV laser irradiation are 0.3, 0.5, 0.7, 1, 1.2, and 1.5 μs for panels b−g, respectively.

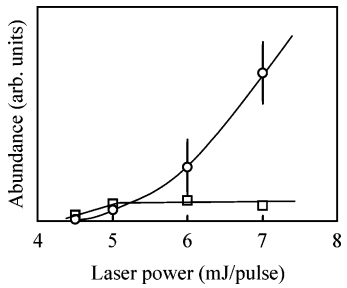

Figure 6. Plot of the abundance of the fast (□) and the slow (○) components in flight-time distributions shown in Figure 3 as a function of the incident IR laser power. The scale for the fast component is enlarged by a factor of 10. The solid curves are eye guides.

pulse), but the abundance of the slow component increases more significantly than that of the fast component after the laser power exceeds the threshold value. Figure 7 shows the floating velocity, *V*, of each component as a function of the power of the IR laser. The floating velocities of the fast and the slow components increase with increase in the laser power in the ranges of 1400−2300 and 780−1500 m/s, respectively. Figure 8 shows the translational temperature of the fast and the slow components as a function of the IR laser power. The fast and the slow components have the translational temperatures of ∼740 and ∼3000 K, respectively, which are almost independent of the incident IR laser power. Figure 9 shows the values of λ (the reciprocal of the average masses of the fast and the slow components) as a function of the incident IR laser power. The fast component has a larger λ value than the slow component, and the λ values of both the components are almost independent of the incident IR laser power. In other words, the average size of the slow components is larger than that of the fast component and the average sizes of both the components are independent of the power of the IR laser.

5. Discussion

5.1. Ejection of Large Neutral Clusters. As described in the previous section, neutral species were produced and detected directly by the Daly detector under irradiation of the IR laser onto the liquid beam of water. These neutral species are considered to be neutral water clusters, $(H_2O)_n$, having a kinetic energy larger than the work function of the aluminum target of the Daly detector. Actually, Even and co-workers have reported that neutral clusters with masses of more than 1000 amu are ionized in collision with an aluminum surface at a velocity higher than 1 km/s, at which the kinetic energies of the clusters exceed the work function of the aluminum surface.[26,27] It is proved that clusters with masses of more than 1000 amu are actually produced in the gas phase as shown in Figure 4. Figure 4 also shows that the average size of the observed cluster ions increases with an increase in the IR laser power up to 4 mJ/pulse, and levels off above 4 mJ/pulse. This result suggests that different ejection mechanisms operate in the high and low laser power ranges; the mechanism switches at ∼4 mJ/pulse. In reality, the neutral clusters start to be observed at the laser power of 4.5 mJ/pulse as shown in Figure 6.

It is likely that the clusters belonging to the fast and the slow components are ejected from the surface and the inside regions of the liquid beam, respectively, because those from the surface

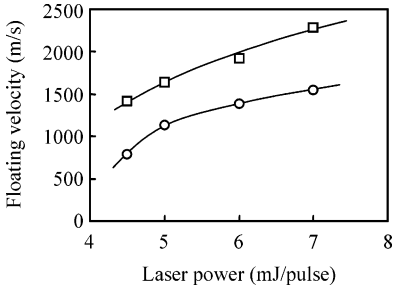

Figure 7. Plot of the floating velocities of the fast (□) and the slow (○) components as a function of the incident IR laser power. The solid curves are eye guides.

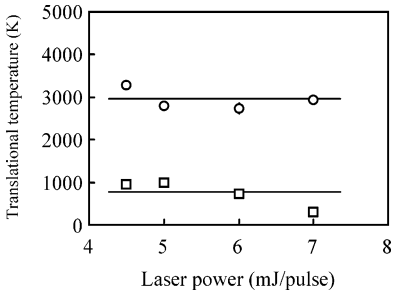

Figure 8. Plot of the translational temperature of the product clusters of the fast (□) and the slow (○) components as a function of the incident IR laser power. The solid lines are eye guides.

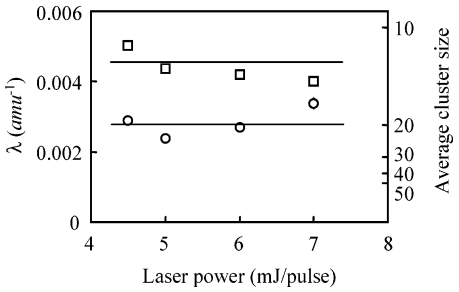

Figure 9. Plot of the values of λ (the reciprocal of the average masses of the fast (□) and the slow (○) components) as a function of the incident IR laser power. The solid lines are eye guides.

region suffer much less collision with any ambient gas than those from the inside. As a result of collision with the ambient gas, the clusters from the inside should gain much more internal energy than those from the surface region. This inference on the ejection scheme is supported by the result that the slow component (clusters from the inside) has a higher translational temperature than the fast component (clusters from the surface) (see Figure 8). On the other hand, the clusters of the fast component originate from the surface, so that the average size of the fast component is smaller than that of the slow component (see Figure 9). This ejection scheme is further supported by the finding that the abundance of the slow component increases more with the IR laser power. More intense IR-laser irradiation is likely to produce clusters from a deeper region of the liquid beam, which is attributed to the clusters of the slow component.

As the power of the IR laser increases, the floating velocity of the neutral clusters increases (Figure 7), whereas the translational temperature and the average size do not change (Figure 8). In other words, the translational energy increases with an increase in the incident IR-laser power, whereas the internal energy of the neutral clusters does not change with the incident IR-laser power. In addition, the translational temperature of the clusters, 3000 K, would be extraordinary high for the water clusters whose internal temperature is much lower. This finding indicates that the water clusters are not produced in the gas phase via evaporation. It is possible that the water clusters are produced by inhomogeneous local heating because of the presence of the start time and the threshold laser power.[28]

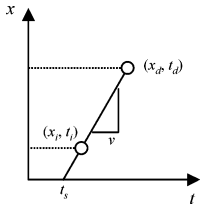

Figure 10. Scheme drawing which explains the procedure for obtaining the start time of the photoionized clusters.

5.2. Retroactive Analysis of Start-Time Distribution. Under irradiation of an intense IR-laser pulse on a liquid beam surface, various chemical species are ejected from the surface due to the ablation by the laser pulse at a delay time after the laser pulse is fired. This delay time is interpreted as a "start time", during which the number density of bubbles formed in a superheated portion of the liquid beam increases up to a critical value. When the number of bubbles reaches the critical value, the superheated portion explodes into pieces (clusters). A liquid beam of a 0.2 M aqueous solution of aniline was used to obtain the start time distribution and the corresponding velocity distribution. Figure 10 shows the procedure for obtaining the start time of the photoionized clusters, t_s, where x and t represent the spatial position (the distance from the liquid beam) and the time elapsed after the IR laser is fired, respectively, x_i represents the spatial position at which the UV ionization laser is fired at time t_i, and x_d represents the position of the detector at which a product arrives at time t_d.

Let us suppose that a cluster is ejected from the liquid beam by an IR laser pulse. The position, x, is expressed in terms of t as

$$x = v(t - t_s) \tag{11}$$

where v represents the velocity of the cluster. The values of v and t_s are obtained from the given values of (x_i, t_i) and (x_d, t_d).

With $x_d = 1.65$ m, one obtains the start-time distribution and the velocity distribution of the photoionized clusters from the flight-time distribution (Figure 5), as shown in Figures 11 and 12, respectively. The error of the start-time distribution is estimated to be ~ 0.1 μs.[29] The start-time distribution consists of a small peak at $t_s \sim 0$ μs and a large peak at $0.1 \leq t_s \leq 1$ μs (see panels a and b of Figure 11 for instance). The small peak appearing at $t_s \sim 0$ μs is assignable to clusters ejected from the surface because of no appreciable time for the clusters to be liberated from the liquid beam. On the other hand, the large peak is attributed to clusters from the inside of the beam because they need a substantial time ($t_s \leq 1$ μs) to be released from the liquid beam; the clusters linger on for a while before they are completely liberated into the gas phase, due to collision with a dense cloud of water vapor in their vicinity. The lingering of the clusters is manifested on the $v-t_s$ relationship depicted in Figure 13, as supported by the decrease of the cluster velocity with t_s. It is considered that the clusters from the surface and the inside of the liquid correspond to the clusters of the fast and the slow components, respectively, because the velocity of the clusters decreases during the lingering process. This cluster ejection scheme is depicted in Figure 14. It looks contradictory that the velocity of the fast component from the surface is smaller than that of the slow component from the inside (see Figure 13). This phenomenon arises from the fact that the UV

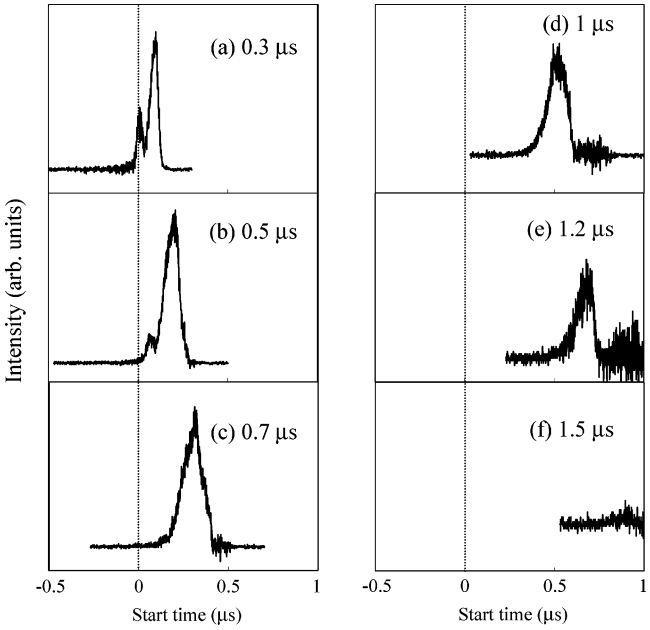

Figure 11. Start-time distributions of photoionized clusters calculated from the flight-time distributions (see Figure 5). The sample solution employed is a 0.2 M aqueous solution of aniline. The panels designated by a, b, c, ... correspond to those designated by a, b, c, ... given in Figure 5.

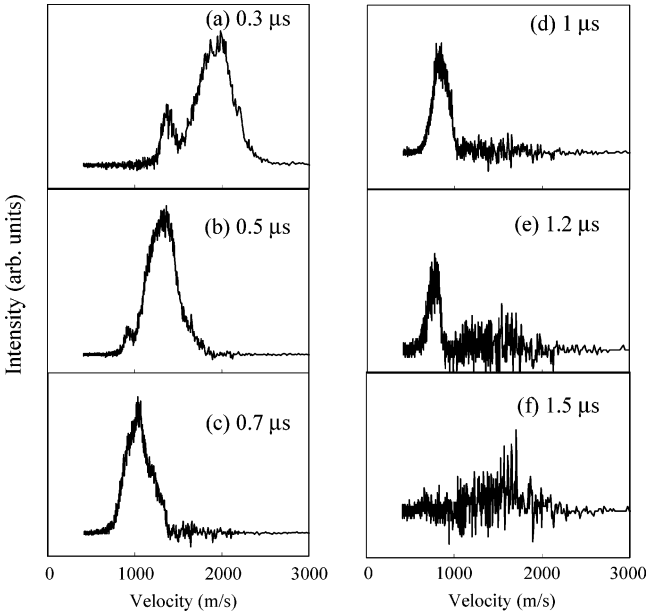

Figure 12. Velocity distributions of the photoionized clusters calculated from the flight-time distributions in Figure 5. The sample solution employed is a 0.2 M aqueous solution of aniline. The panels designated by a, b, c, ... correspond to those designated by a, b, c, ... given in Figures 5 and 11.

laser samples a slow component of the fast component and a fast component of the slow component simultaneously. It is likely that the velocity of the fast component exceeds that of the slow one when the measurement is performed in delay times shorter than 0.3 μs.

6. Conclusion

We investigated the mechanism of laser ablation of a liquid beam of water under irradiation of an intense IR laser by using the start-time distribution of the produced water clusters, which is derived from the flight-time distributions. It was concluded

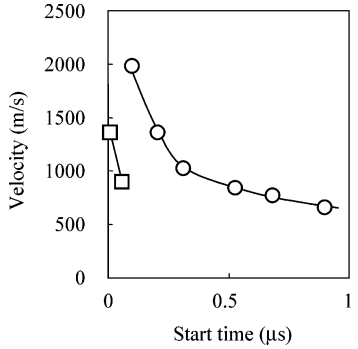

Figure 13. Velocities of two components in the flight-time distribution as a function of the start time, which are obtained from the corresponding peak positions of the start time and the velocity shown in Figures 11 and 12, respectively. The solid curves are eye guides.

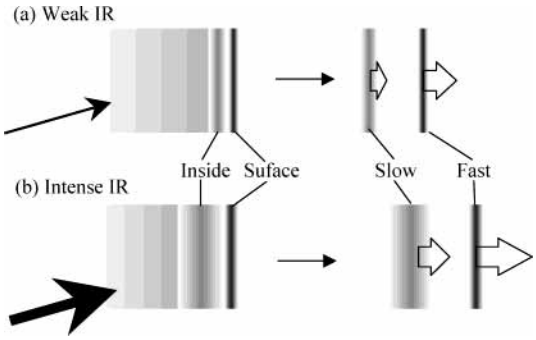

Figure 14. A scheme showing the cluster ejection following IR laser irradiation. The clusters of the fast and the slow components are ejected from the surface and the inside region of the liquid beam, respectively.

that the water clusters are produced from the surface and the inside of the liquid beam. The cluster ejection is not statistical, such as inhomogeneous local heating followed by explosion of the liquid beam. This finding provides an important basis for isolation of large molecules from their aqueous solutions.

Acknowledgment. The authors are grateful to Mr. Yoshihiro Takeda for his assistance in the early stage of the liquid beam. This research was supported by the Special Cluster Research Project of Genesis Research Institute, Inc.

References and Notes

(1) Srinivasan, R.; Ghosh, A. P. *Chem. Phys. Lett.* **1988**, *143*, 546.
(2) Tsuboi, Y.; Fukumura, H.; Masuhara, H. *Appl. Phys. Lett.* **1994**, *64*, 2745.
(3) Tsuboi, Y.; Fukumura, H.; Masuhara, H. *J. Phys. Chem.* **1995**, *99*, 10305.
(4) Hatanaka, K.; Kawao, M.; Tsuboi, Y.; Fukumura, H.; Masuhara, H. *J. Appl. Phys.* **1997**, *82*, 5799.
(5) Hatanaka, K.; Tsuboi, Y.; Fukumura, H.; Masuhara, H. *J. Phys. Chem. B* **2002**, *106*, 3049.
(6) Furlan, A. *Chem. Phys. Lett.* **1997**, *275*, 239.
(7) Furlan, A. *Chem. Phys. Lett.* **1999**, *309*, 157.
(8) Faubel, M.; Schlemmer, S.; Toennies, J. P. *Z. Phys.* **1988**, *D10*, 269.
(9) Faubel, M.; Kisters, Th. *Nature* **1989**, *339*, 527.
(10) Kleinekofort, W.; Avdiev, J.; Brutschy, B. *Int. J. Mass Spectrosc.* **1996**, *152*, 135.
(11) Kleinekofort, W.; Schweitzerm M.; Engels, J. W.; Brutschy, B. *Int. J. Mass Spectrosc.* **1996**, *156*, 195.
(12) Kleinekofort, W.; Schweitzerm M.; Engels, J. W.; Brutschy, B. *Int. J. Mass Spectrosc.* **1997**, *163*, 1.
(13) Sobott, F.; Kleinekofort, W.; Brutschy, B. *Anal. Chem.* **1997**, *69*, 3587.
(14) Sobott, F.; Wattenberg, A.; Barth, H.; Brutschy, B. *Int. J. Mass Spectrosc.* **1999**, *185*, 271.
(15) Wattenberg, A.; Sobott, F.; Barth, H.; Brutschy, B. *Int. J. Mass Spectrosc.* **2000**, *203*, 49.

(16) Charvat, A.; Lugovoj, E.; Faubel, M.; Abel B. *Eur. Phys. J. D* **2002**, *20*, 573.
(17) Horimoto, N.; Kohno, J.; Mafuné, F.; Kondow, T. *J. Phys. Chem. A* **1999**, *103*, 9569.
(18) Horimoto, N., Kohno, J.; Mafuné, F.; Kondow, T. *Chem. Phys. Lett.* **2000**, *318*, 536.
(19) Kohno, J.; Mafuné, F.; Kondow, T. *J. Phys. Chem. A* **2001**, *105*, 8939.
(20) Kohno, J.; Mafuné, F.; Kondow, T. *Chem. Lett.* **2002**, 562.
(21) Michaelson, H. B. *J. Appl. Phys.* **1977**, *48*, 4729.
(22) Assume that a cluster with a mass M and with a velocity V releases a molecule with a mass of m, kinetic energy and momentum are conserved as

$$\frac{1}{2}MV^2 = \frac{1}{2}mv^2 + \frac{1}{2}(M - m)v'^2 \quad \text{(a)}$$

$$MV = mv + (\mathrm{M} - m)v' \quad \text{(b)}$$

where v and v' are the velocities of the released molecule and the product cluster, respectively. Equations a and b are solved as

$$V = v = v' \quad \text{(c)}$$

X which means that the velocity of the cluster is conserved even after unimolecular dissociation.

(23) In reality, the detection efficiency increases and levels off with increase in the kinetic energy near the work function of an aluminum metal. In a pulse-counting measurement, the detection efficiency changes simply the heights of signal pulses, but not the number of signal pulses. In other words, the number of clusters is properly detected *when the kinetic energy of the clusters exceeds the work function*.
(24) We have measured the size distribution of the product clusters, $A(n)$, from their spatial distributions by changing the focal position of the UV laser from the liquid beam to the direction away from the liquid beam, where the UV laser is used to ionize the chromophores embedded in the clusters. The result reveals that the size of the clusters produced by IR laser ablation of the liquid beam decreases exponentially with their masses.
(25) The peaks are assigned to the fast and the slow components as follows: The abundance of the fast component decreases with an increase in the laser power as shown in panels a and b of Figure 2. It is concluded that the more abundant component is assigned to the slow component shown in panels c and d.
(26) Even, U.; de Lange, P. J.; Jonkman, H. Th.; Kommandeur, J. *Phys. Rev. Lett.* **1986**, *56*, 965.
(27) Vostrikov, A. A.; Zadorozhny, A. M.; Dubov, D. Yu.; Witt, G.; Kazakova, I. V.; Bragin, O. A.; Kazakov, V. G.; Kikhtenko, V. N.; Tyutin, A. A. *Z. Phys. D* **1997**, *40*, 542.
(28) Park, B.-S.; Biswas, A.; Armstrong, R. L. *Opt. Lett*. **1990**, *15*, 206.
(29) The dominant error of the start-time distribution originates from the error in the distance measurement, which is considered to be in a range of the diameter of the UV laser ($\sim$100 μm). It turns out that the error of the start-time distribution is $\sim$0.1 μs.